A Flexible Black-Box Model for Conducted Emission Predictions with Different Switching Frequencies

Lu Wan, Xinglong Wu, Xiaokang Liu, Flavia Grassi, Giordano Spadacini, Sergio A. Pignari
Dept. of Electronics, Information and Bioengineering
Politecnico di Milano
Milan, Italy
lu.wan@polimi.it

***Abstract*—Black-box modeling technique is an efficient approach to represent the electromagnetic interference behavior of power converters, whose presence may cause malfunctioning in adjacent electronic devices. Although developing a black-box model is simpler and less demanding than extracting an explicit circuit model, model effectiveness is limited to certain operating conditions, such as a fixed modulation strategy. In this work, a flexible black-box model is proposed, which can be effectively used for prediction also in case of different modulation conditions without requiring a new estimation of model parameters if modulation parameter (such as the switching frequency) changes. Flexibility is achieved by modeling time-domain noise waveforms using an analytical curve-fitting model or an autoregressive model, whose accuracy is compared in time and frequency domain. The proposed model is experimentally verified on a boost converter operated with different switching frequencies.**

Keywords—EMI, conducted emissions, black-box modeling, autoregressive model, curve-fitting, power converters

I. INTRODUCTION

Electromagnetic interference (EMI) caused by power converters is a major concern in the design and operation of electrical and electronic systems [1]. EMI can cause malfunctions or failures of sensitive devices, as well as interfere with the operation of powerline communications (PLC) [2]. For system-level EMI analysis, an accurate EMI model of power converters is essential in terms of accuracy and flexibility. Particularly, the flexibility of EMI model in modulation parameters is important to assess the worst-case scenario and to evaluate possible co-existence issues with other systems.

The available modeling approaches can be classified into two main categories: circuit model and black-box (or behavioral) model. Circuit modeling is based on a detailed representation of the internal structure including not only the electrical components and their interconnections, but also the parasitic paths responsible for the couplings of high-frequency noise. Although complex, the circuit model is flexible and can be effortlessly adapted to different operating conditions. However, a thorough knowledge of the internal structure of the converter is not always available, and values of parasitics can hardly be determined. In addition, circuit models may result in time-consuming simulations, which may also lead to non-convergence problems [3].

Conversely, black-box modeling does not require a detailed knowledge of the internal structure of the converter(s), which is treated as a linear time-invariant (LTI) system. The obtained models are simpler to be developed than circuit models. Several techniques have been proposed to identify and validate black-box models for power converters. A comparison of different modeling approaches in terms of advantages, limitations, and requirements can be found in [4]. Black-box modeling of power converters can facilitate engineers' efforts to design EMI filters and investigate the aggregated emissions in a multiple converter system [5]. However, a drawback of conventional black-box modeling strategies is that the obtained model is valid for the specific modulation strategy used to extract model parameters. If modulation settings (such as the switching frequency) change, new measurements are required to extract relevant model parameters assuring reliable prediction of conducted emissions (CE).

In this work, based on the analysis of the time-domain waveform of CE, an alternative black-box approach able to predict the CE of power converters under different switching frequencies is proposed and experimentally verified on a setup involving a boost converter. To this end, two mathematical models for representing the converter CE are implemented and compared: the analytical curve-fitting model (thereinafter called fitted model) and the autoregressive (AR) model. Compared with traditional black-box modeling approaches, the proposed approach avoids the need to repeat measurement when the modulation changes.

The rest of the paper is organized as follows. In Section II, the experimental setup to extract black-box model parameters and an example of results are presented. In Section III, CE time-domain waveform is investigated and modeled by two mathematical models. In Section IV, the proposed procedure is presented, compared with the conventional method, and used to model a boost converter for CE prediction. Eventually, conclusions are drawn in Section V.

II. BLACK-BOX MODEL DEVELOPMENT

According to [6], black-box modeling of power converters involves two measurement steps. First, the parameters of the passive part (admittance matrix) are characterized by VNA measurement. Then, the active part (current noise sources) are extracted from measurement of the CE exiting the converter in a suitable test setup. In a previous study, the setup of active part employing a three-phase line impedance stabilization network (LISN) was proposed to model the ac output of a PV-inverter system [7]. In this work, the modeling procedure using LISN is adjusted to unterminated condition for both the input and output side of a boost converter (evaluation board: KIT-CRD-3DD065P).

In the first step for passive part evaluation, the scattering parameters (S-parameter) of the boost converter are measured by connecting a four-port VNA to the four terminals of the converter (two input and two output ports). The converter is kept at a constant distance from the ground plane for reproducibility during all measurement campaigns. Due to the

This project has received funding from the European Union's Horizon 2020 research and innovation programme under the Marie-Skłodowska-Curie grant agreement No 812753.

masking effects of the input/output capacitors, the measured S-parameters when the MOSFET is in ON and OFF status do not show significant deviations in the measured frequency range (from 9 kHz to 100 MHz). This finding proves that the boost converter under analysis can be approximately regarded as a LTI system, hence the black-box modeling technique is applicable [8].

The second step to evaluate the active part of the black-box model is shown in Fig. 1. The dc power supply set as 10 V provides power to the input of the boost converter through a two-phase LISN, whose bandwidth, specified in standard DO-160G, is from 10 kHz to 400 MHz. The converter driven by a PWM signal (duty cycle: $D = 0.5$, switching frequency sf = 20 kHz) boosts the output voltage level for a resistive load (100 Ω) to 20 V. Some main parasitic components to the ground plane in the setup are labeled in red. A four-channel oscilloscope simultaneously measures time-domain waveforms of voltages at both input and output sides of the boost converter, which can be converted into frequency-domain spectra through the Fast Fourier Transform (FFT). Channels 1 and 2, with input impedances set as $Z_0 = 50$ Ω, are connected to the RF receiver ports of the LISN, while channels 3 and 4, with high input impedance (1 MΩ), are used to measure two terminals at the load side. The spectra of the current noise sources (I_{s1}, I_{s2}, I_{s3}, and I_{s4}) can be obtained as:

$$\begin{bmatrix} I_{s1} \\ I_{s2} \\ I_{s3} \\ I_{s4} \end{bmatrix} = \begin{bmatrix} I_1 \\ I_2 \\ I_3 \\ I_4 \end{bmatrix} + \boldsymbol{Y_{DUT}} \begin{bmatrix} V_1 \\ V_2 \\ V_3 \\ V_4 \end{bmatrix} \tag{1}$$

where, $\boldsymbol{Y}_{\mathbf{DUT}}$ (associated with the passive part of the model) is the 4×4 admittance matrix derived from the measured S-parameter in the first step. V_1, V_2, I_1, I_2 , and V_3, V_4, I_3, I_4 are Fourier coefficients of terminal voltages and currents at the input and output side of the converter, respectively (see Fig. 1), which are computed as follows:

$$\begin{bmatrix} V_1 \\ V_2 \\ I_1 \\ I_2 \end{bmatrix} = \boldsymbol{ABCD_{LISN}} \begin{bmatrix} V_{1m} \\ V_{2m} \\ V_{1m}/Z_0 \\ V_{2m}/Z_0 \end{bmatrix} \tag{2}$$

$$\begin{cases} \begin{bmatrix} V_3 \\ V_4 \end{bmatrix} = \begin{bmatrix} V_{3m} \\ V_{4m} \end{bmatrix} \\ \begin{bmatrix} I_3 \\ I_4 \end{bmatrix} = \boldsymbol{Y_{Load}} \begin{bmatrix} V_3 \\ V_4 \end{bmatrix} \end{cases} \tag{3}$$

where, V_{1m}, V_{2m} , V_{3m}, and V_{4m} are the Fourier coefficients of the time-domain waveform measured by the oscilloscope. $\boldsymbol{ABCD}_{\mathbf{LISN}}$ is the 4×4 ABCD matrix of the LISN, and $\boldsymbol{Y}_{\mathbf{load}}$ is the 2×2 admittance matrix of the load, and both are obtained from the S-parameters measured by the VNA.

The obtained entries of the admittance matrix and noise source vector representing the boost converter are plotted in Fig. 2. For better visualization, only the first row of the admittance matrix $\boldsymbol{Y}_{\mathbf{DUT}}$ is plotted here. Besides, the peaks of the current sources I_{s2}, I_{s3}, and I_{s4} are compared with the spectrum of I_{s1}.

When the modulation changes, for instance, the switching frequency changes to 100 kHz, the passive part of the model remains the same, while the noise sources derived for sf = 20 kHz cannot be longer used to predict the CE exiting the boost converter, and new measurements are theoretically required to evaluate the entries of the noise current source vector.

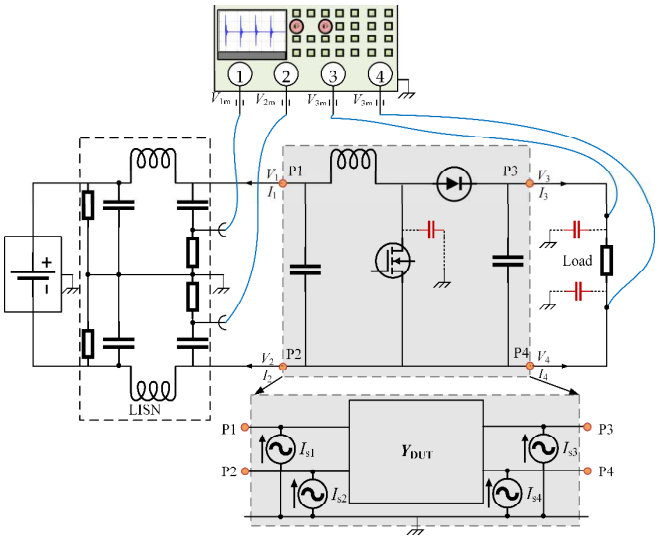

Fig. 1. Principle drawing of the measurement setup to evaluate the active part of black-box model.

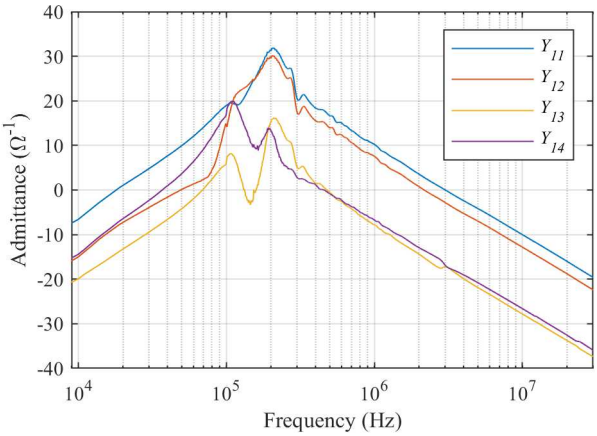

(a)

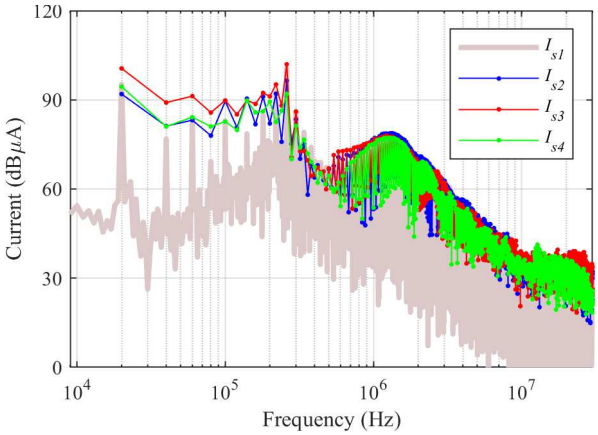

(b)

Fig. 2. (a) Selected entries of the admittance matrix $\boldsymbol{Y}_{\mathbf{DUT}}$ and (b) spectra of the current noise sources.

III. Time-Domain Analysis of Conducted Emissions

In this Section, the transient characteristics of the CE waveforms exiting the boost converter under different

modulation conditions (taking the switching frequency as an example) are investigated by the use of analytical models.

A. General Waveform of Noise Signals

A general representation of the noise waveform exiting the converter can be achieved by resorting to periodic trains of trapezoid-shaped pulses with ringing signals. An example is shown in Fig. 3a, which represents the noise waveform of a PWM signal with switching frequency sf and duty cycle D, whose period and pulse width can be obtained as $T_{sf} = 1/sf$, and DT_s, respectively. As shown in Fig. 3a, ringing happens as the PWM signal moves from one logic level to another with overshoot and undershoot after the pulse rises and falls, respectively.

This general noise representation can be treated as the linear combination of three waveforms: the trapezoid-shaped pulse with superimposed overshoot and undershoot waveforms (see Fig. 3b). Consequently, the corresponding Fourier series can be written as a linear combination of the Fourier series of each decomposed waveform. A detailed derivation of the Fourier series of a general noise waveform can be found in [9].

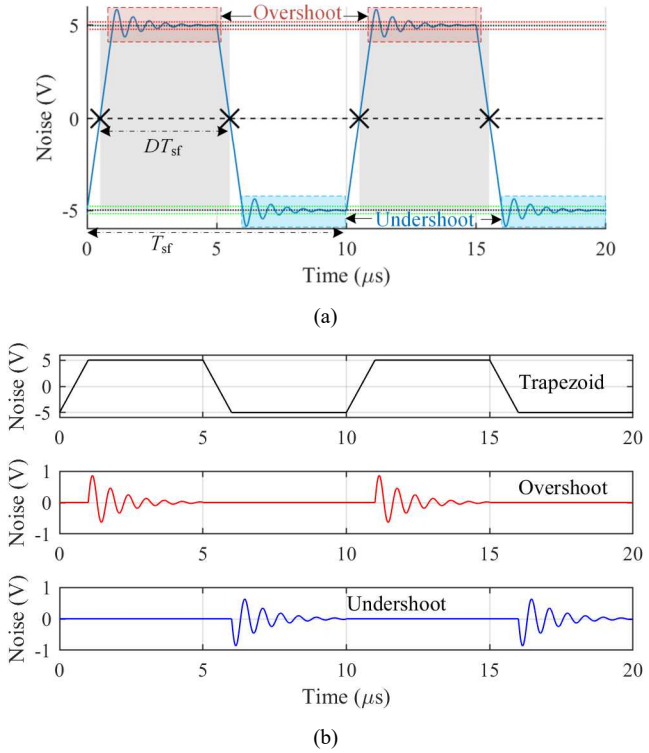

Fig. 3. (a) General representation of a noise waveform and (b) its decomposition into trapezoidal, overshoot, and undershoot waveforms.

B. Noise under Different Switching Frequencies

The noise exiting port 1 of the boost converter is measured by an oscilloscope with the converter operated with two different switching frequencies (20 kHz and 40 kHz), and the obtained waveforms are compared in Fig. 4. The corresponding spectra are obtained by FFT with an interval of one millisecond and 1 GHz sampling frequency.

Comparison of the noise spectra reveals that the first peak occurs at the switching frequency, as expected, and the spectra envelopes resemble the same pattern, e.g., both reach the peak around 1.3 MHz. Apart from that, it is not easy to associate the two spectra analytically. Instead, the time-domain waveforms show a straightforward correlation. In Fig. 4, the waveforms are compared in the same time interval (50 µs), which offers one period of waveform with sf = 20 kHz and two periods for the case with sf = 40 kHz. Both waveforms can be decomposed into overshoot and undershoot parts, which occurs at half-period intervals.

To further compare the ringing signals, both overshoot and undershoot waveforms (considering 5 µs time interval) under two switching frequencies are compared in Fig. 5. The indicator one minus the normalized root-mean-square error (1-NRMSE) shown in percentage in the legend, represents how closely the two time-series data match. For both overshoot and undershoot cases, two waveforms under different switching frequencies are nearly equal. The comparison of the spectra confirms the possibility of interchanging the ringing signals between different modulation cases of switching frequency, with other parameters of operating conditions fixed (such as input voltage, load, duty cycle, etc.). In fact, the parasitic inductance and capacitance of MOSFET modules and PCB transmission path are responsible for the ringing effects. For the boost converter in this work, the ringing signal does not change significantly when the switching frequency varies from 10 kHz to 100 kHz. In other words, once the ringing signals are obtained from one measurement for a specific switching frequency, approximate time-domain waveforms for a different switching frequency can be retrieved from proper combination of the overshoot and undershoot waveforms.

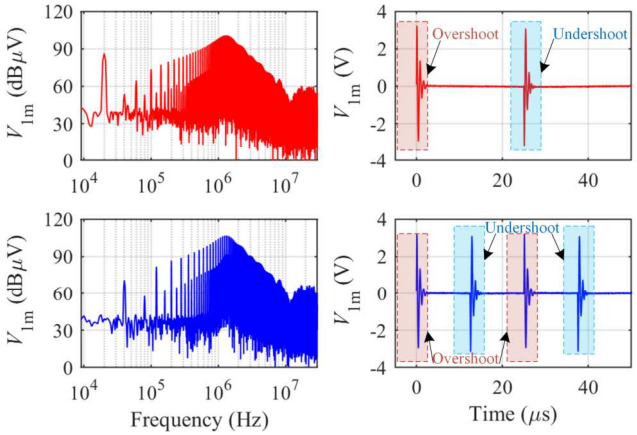

Fig. 4. Waveform spectra of the noise signal V_{1m} with switching frequency 20 kHz (top two panels) and 40 kHz (bottom two panels).

C. Analytical Modeling of Ringing Waveforms

Although the comparison in Fig. 5 shows that the overshoot/undershoot waveforms are independent on the switching frequency, other operating conditions (such as input voltage, load, and duty cycle) may impact on the ringing waveforms significantly. Therefore, it is necessary to model the ringing waveforms analytically. To this end, two analytical approaches are proposed to model the ringing waveforms: The fitted model and the AR model.

The former approach consists in applying curve-fitting to the ringing waveforms. To this end, the following analytical expression is proposed:

$$y(t) = Ate^{-\pi\frac{f}{Q}(t-t_1)}\sin[2\pi f(t-t_1)] \qquad (3)$$

which involves four parameters: the amplitude A, the damping factor Q, the frequency f in MHz, and a time shift t_1 in µs. The

expression in (3) contains: (a) a sinusoidal signal representative for the waveform oscillating part; and (b) an exponential part accounting for damping. This expression is similar to that of the damped sinusoidal waveform defined by the standard [10] but with time-variant amplitude.

Optimization of the four parameters in (3) is carried out by a *pattern search* strategy (implemented in Matlab) to fit each waveform. If the overshoot and undershoot waveform of V_{1m} (obtained with 20 kHz switching frequency) is considered as an example, optimal values of these parameters are those collected in Table I.

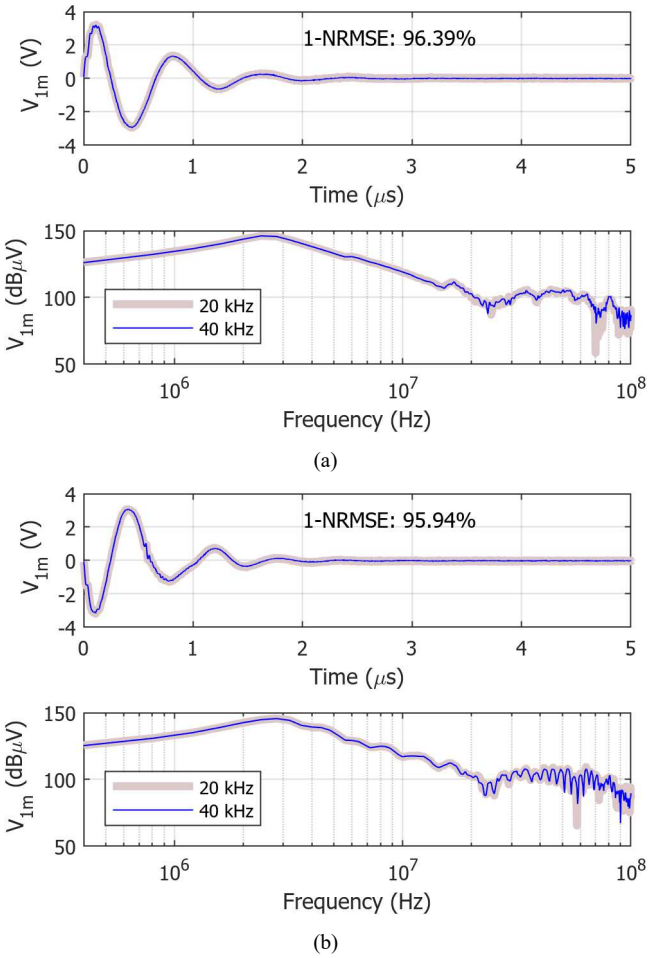

Fig. 5. Comparison of waveforms and spectra under two different switching frequency (20 kHz and 40 kHz) for the (a) overshoot and (b) undershoot respectively.

TABLE I. PARAMETERS OF THE ANALYTICAL FITTED MODEL

Waveform	Parameters			
	A	Q	f (MHz)	t_1 (μs)
Overshoot	3.0082	0.9563	1.245	0.6588
Undershoot	-3.1427	0.9521	1.3314	0.6221

An alternative approach is to use the AR model to describe the ringing signals. The AR model is a statistical model that is used to describe a time series in which the current value is a linear function of past values, plus some random noise. The general form of an AR model is:

$$y(t) = c + a_1 y(t-1) + \cdots + a_p y(t-p) + \varepsilon(t) \quad (4)$$

where $y(t)$ is the current value of the time series, c is a constant term, a_1, …, a_p are coefficients, $y(t–1)$,…, $y(t–p)$ are past values of the time series, and $\varepsilon(t)$ is a random noise term. The parameter p denotes the order of the model.

In general, the order of the AR model determines the number of past values that are used to predict the current value. A higher-order model will have more terms and may be able to capture more complex dynamics in the time series, but it may also be more prone to overfitting. To select a good order for the AR model, the Rissanen's Minimum Description Length (MDL) principle is applied to achieve a trade-off between fitting accuracy and model complexity.

TABLE II. PERFORMANCE COMPARISON OF TWO MODELS

Metrics	Fitted model		AR model	
	Overshoot	Undershoot	Overshoot	Undershoot
MSE	0.0126	0.0139	0.0001341	0.0001484
1-NRMSE	86.2%	84.62%	98.6%	98.5%
Number parameter	4	4	36	34

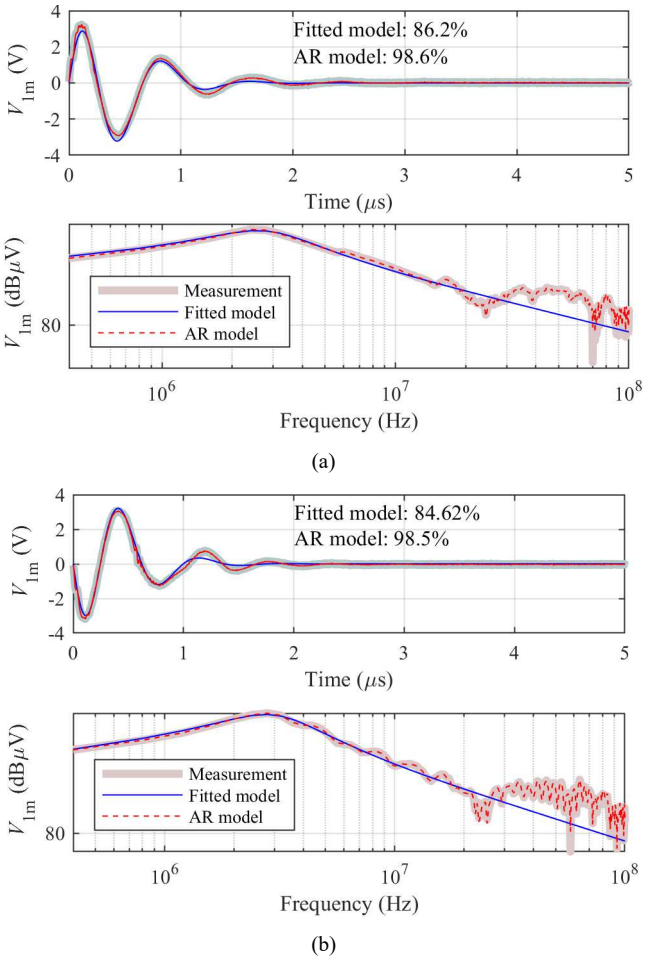

Fig. 6. Waveform and spectra reconstruction (20 kHz switching frequency) for the (a) overshoot and (b) undershoot, respectively, with 1-NRMSE indicator for comparison.

The comparison is based on the dataset of overshoot and undershoot waveforms measured at LISN output (V_{1m}) under 20 kHz switching frequency. The mean squared error (MSE), 1-NRMSE and number of parameters of model are selected as metrics in Table II. Besides, the accuracy of the two models

in reconstructing the original waveform and its spectrum is compared in Fig. 6.

The comparison shows that the AR model outperformes the curve-fitting analytical model in terms of MSE and 1-NRMSE. Namely, the AR model provides lower MSE and higher 1-NRMSE, indicating a better fitting of measurement data. This conclusion is confirmed also in terms of spectra, which reveal that the fitted model cannot provide accurate reconstruction above 20 MHz. However, the AR model requires higher orders than the fitted model, which needs four parameters only.

IV. Flexible Black-Box Model

In this Section, a flexible black-box modeling technique is proposed based on the fitted and AR models.

A. Proposed Modeling Procedure

The objective here is to develop a flexible procedure, which avoids the need for new measurements every time modulation parameters of the converter, e.g., the switching frequency, change. The approach is based on the analytical fitting procedures presented in the previous section, and, with respect to traditional black-box modeling approachs, encompasses the steps in Fig. 7.

In both cases, the passive part of the model is extracted as the first step by resorting to S-parameter measurement at the ports of the converter switched off. Hence, the validity of the LTI assumption should be verified as mentioned in Section II, or by comparing the differential mode impedance of the converter measured with the converter switched ON and OFF, for instance by the inductive coupling method in [11].

If the LTI assumption is verified, the noise sources for case 1 with $sf=f_1$ can be derived based on CE measurement as described in Section II. To derive the black-box model for a different switching frequency $sf=f_2$ (case 2), instead of repeating the measurements, the already available noise waveforms (case 1) are decomposed into overshoot and undershoot waveforms, which are then post-processed by the curve-fitting method or the AR model.

CE waveforms for case 2 are then reconstructed based on the adopted analytical model, and the noise sources of the balck-box model are eventually extracted from those post-processed waveforms.

B. Comparison of Conducted Emissions and Noise Sources

This section compares two results of the flexible black-box model with the conventional method (used as reference), in terms of the reconstructed CE waveform and its spectrum, and the active part of black-box model. As an example, the switching frequency is set as 20 kHz and 100 kHz for case 1 and 2, respectively.

In the proposed procedure, the CE noise waveforms of case 2 are reconstruted for a period of 1 ms. If channel 1 is considered as an example, the first period (10 µs) is plotted in Fig. 8a, and compared with measurement data. As expected, the AR model fits the data better than the fitted model in terms of the 1-NRMSE. Besides, the spectra of the reconstructed one-millisecond data in Fig. 8b show that both analytical models can provide good accuracy below 10 MHz. Moreover, the AR model can even fit the data up to 100 MHz.

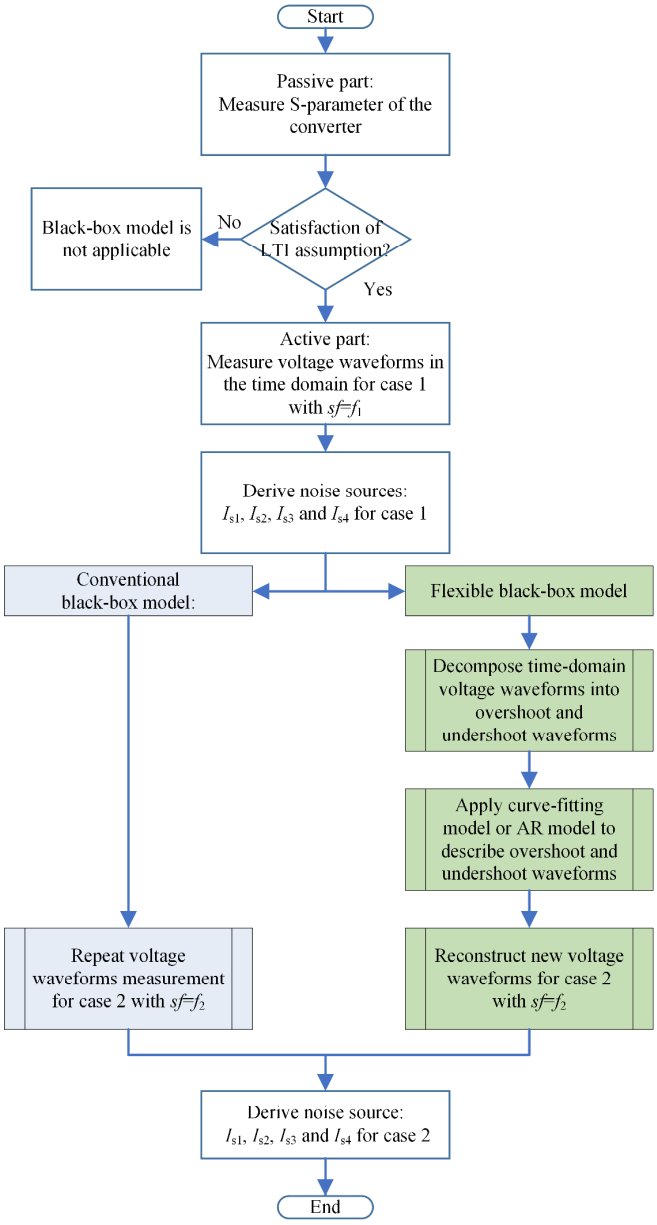

Fig. 7. Conventional vs proposed black-box modeling procedures: Comparison of the work-flows to be followed in order to derive the model of the same converter operated with two different switching frequencies f_1 and f_2.

The current sources of the proposed black-box model for case 2 is derived by the curve-fitting and the AR model. In Fig. 8c, the current sources (I_{s1}) from the aforesaid two models are compared here with the one from the conventional method. The comparisons show that both analytical methods can correctly predict peak frequencies, yet avoiding the need to repeat measurement. However, the fitted model is unable to provide accurate results above 10 MHz, while the AR model is still applicable up to 100 MHz.

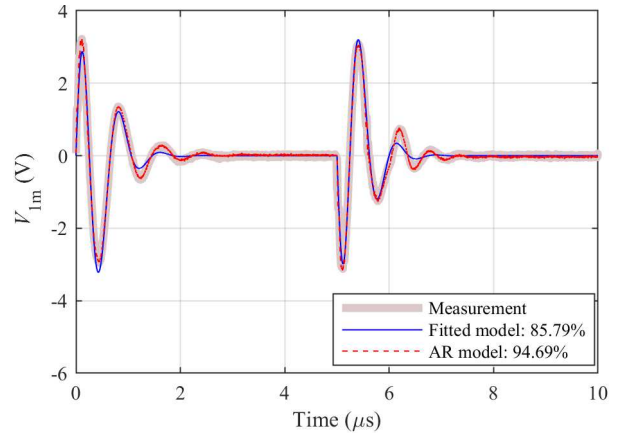

(a)

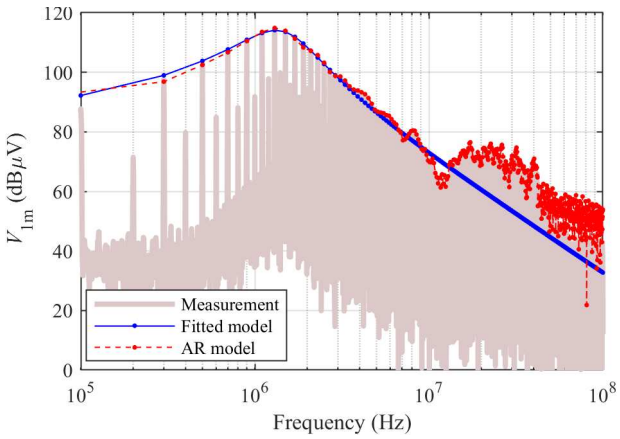

(b)

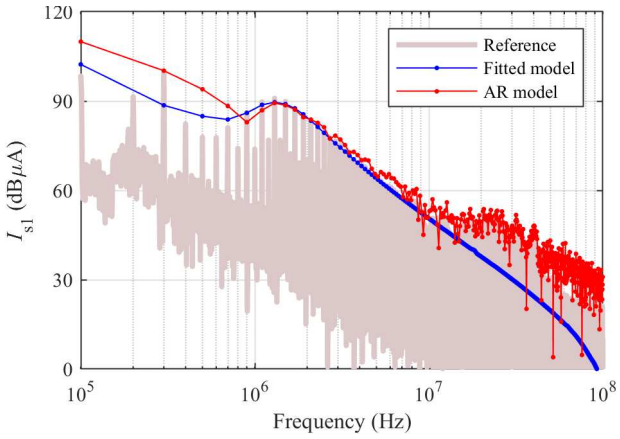

(c)

Fig. 8. Comparison of flexible black-box model (fitted and AR model) with the conventional method (measurement) for case 2 with f_2=100 kHz, in terms of (a) reconstructed noise waveforms and its (b) CE spectra of channel 1 (V_{1m}), and (c) the noise source I_{s1}.

V. Conclusion

This work proposed a flexible black-box modeling procedure based on the time-domain analysis and modeling of noise waveforms. This proposed approach can derive the black-box model for a new modulation case without the requirement of extra measurements. The curve-fitting and AR models were proposed to describe the overshoot and undershoot waveforms. The AR model outperforms accuracy, especially at high frequencies, but it requires more parameters. The fitted model only requires optimizing four parameters, but the accuracy is degraded above 10 MHz. Overall, the proposed black-box modeling procedure proved to be able to provide good CE prediction accuracy in a wide frequency range without involving extra measurements even the switching frequency changes.

References

[1] A. E. Shadare, M. N. O. Sadiku, and S. M. Musa, "Electromagnetic compatibility issues in critical smart grid infrastructure," *IEEE Electromagn. Compat. Mag.*, vol. 6, no. 4, pp. 63–70, 2017.

[2] A. H. Beshir *et al.*, "Influence of Random Modulated Power Converter on G3 Power Line Communication," *Applied Sciences*, vol. 12, no. 11, p. 5550, May 2022.

[3] F. A. Kharanaq, A. Emadi, and B. Bilgin, "Modeling of Conducted Emissions for EMI Analysis of Power Converters: State-of-the-Art Review," *IEEE Access*, vol. 8, pp. 189313–189325, 2020.

[4] L. Wan *et al.*, "Black-box Modeling of Converters in Renewable Energy Systems for EMC Assessment: Overview and Discussion of Available Models," *Chin. J. Electr. Eng.*, vol. 8, no. 2, pp. 13–28, Jun. 2022.

[5] T. J. Donnelly, S. D. Pekarek, D. R. Fudge and N. Zarate, "Thévenin Equivalent Circuits for Modeling Common-Mode Behavior in Power Electronic Systems," in *IEEE Open Access Journal of Power and Energy*, vol. 7, pp. 163-172, 2020.

[6] G. Spadacini, F. Grassi, D. Bellan, S. A. Pignari, and F. Marliani, "Prediction of Conducted Emissions in Satellite Power Buses," *International Journal of Aerospace Engineering*, vol. 2015, pp. 1–10, 2015.

[7] L. Wan et al., "Black-Box Modelling of Low-Switching-Frequency Power Inverters for EMC Analyses in Renewable Power Systems," *Energies*, vol. 14, no. 12, p. 3413, 2021.

[8] H. Bishnoi, A. C. Baisden, P. Mattavelli, and D. Boroyevich, "Analysis of EMI Terminal Modeling of Switched Power Converters," *IEEE Transactions on Power Electronics*, vol. 27, no. 9, pp. 3924–3933, Sep. 2012.

[9] C. R. Paul, R. C. Scully, and M. Steffka, Introduction to electromagnetic compatibility, Third edition. Hoboken, NJ, USA: Wiley, 2022.

[10] X. Liu, F. Grassi, F. Trotti, and W. Hirschi, "Behavioral Modeling of an Off-the-Shelf Damped Sinusoidal Transient Generator," *IEEE Lett. on Electromagn. Compat. Pract. and Appl.*, vol. 4, no. 3, pp. 56–60, Sep. 2022.

[11] L. Wan, S. Negri, G. Spadacini, F. Grassi, and S. A. Pignari, "Enhanced Impedance Measurement to Predict Electromagnetic Interference Attenuation Provided by EMI Filters in Systems with AC/DC Converters," *Applied Sciences*, vol. 12, no. 23, p. 12497, Dec. 2022.